Article

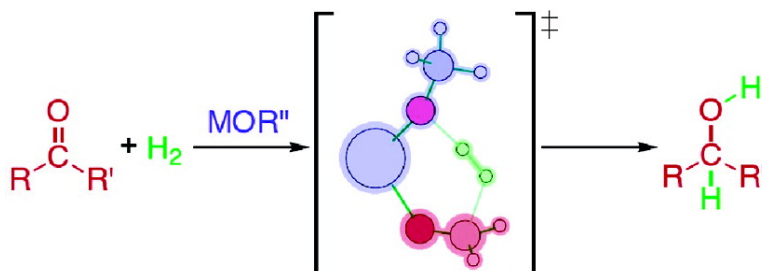# Base-Catalyzed Hydrogenation: Rationalizing the Effects of Catalyst and Substrate Structures and Solvation

Bun Chan, and Leo Radom

More About This Article

Additional resources and features associated with this article are available within the HTML version:

- Supporting Information
- Links to the 10 articles that cite this article, as of the time of this article download
- Access to high resolution figures
- Links to articles and content related to this article
- Copyright permission to reproduce figures and/or text from this article

View the Full Text HTML

J|A|C|S

A R T I C L E S

Base-Catalyzed Hydrogenation: Rationalizing the Effects of Catalyst and Substrate Structures and Solvation

Bun Chan* and Leo Radom*

Contribution from the School of Chemistry, University of Sydney, Sydney, NSW 2006, Australia

Received August 18, 2004; E-mail: chan_b@chem.usyd.edu.au; radom@chem.usyd.edu.au

Abstract: Ab initio molecular orbital calculations have been used to study the base-catalyzed hydrogenation of carbonyl compounds. It is found that these hydrogenation reactions share many common features with S_N2 reactions. Both types of reactions are described by double-well energy profiles, with deep wells and a low or negative overall energy barrier in the gas phase, while the solution-phase profiles show very shallow wells and much higher barriers. For the hydrogenation reactions, the assembly of the highly ordered transition structure is found to be a major limiting factor to the rate of reaction. In the gas phase, the overall barriers for reactions catalyzed by Group I methoxides increase steadily down the group, due to the decreasing charge density on the metal. On the other hand, for Group II and Group III metals, the overall barriers decrease down the group, which is attributed to the increasing ionic character of the metal−oxygen bond. The reaction with $B(OCH_3)_3$ has an exceptionally high barrier, which is attributed to π-electron donation from the oxygen lone pairs of the methoxy groups to the formally vacant p orbital on B, as well as to the high covalent character of the B−O bonds. In solution, these reactivity trends are generally the opposite of the corresponding gas-phase trends. While similar barriers are obtained for reactions catalyzed by methoxides and by *tert*-butoxides, reactions with benzyloxides have somewhat higher barriers. Aromatic ketones are found to be more reactive than purely aliphatic ketones. Moreover, comparison between catalytic hydrogenation of 2,2,5,5-tetramethylcyclopentanone and pivalophenone shows that factors such as steric effects may also be important in differentiating their reactivity. Solvation studies with a wide range of solvents indicate a steady decrease in barrier with decreasing solvent dielectric constant, with nonpolar solvents generally leading to considerably lower barriers than polar solvents. In practice, a good balance between polarity and catalyst solubility is required in selecting the most suitable solvent for the base-catalyzed hydrogenation reaction.

Introduction

Hydrogenation is an important chemical reaction in industrial processes and organic synthesis. Most hydrogenation reactions are catalyzed by transition-metal complexes, both in synthetic chemistry[1] and in biological systems.[2] For instance, compounds that contain platinum-group metals have been used extensively in the hydrogenation of fats in the food industry.[3] In contrast to transition-metal-catalyzed hydrogenations, catalytic hydrogenation without transition metals is much less prominent. Among such studies, it has been found that benzophenone undergoes catalytic hydrogenation in the presence of potassium *tert*-butoxide at high temperatures and H_2 pressure.[4] A recent elegant paper by Berkessel et al. has revealed many mechanistic details on this type of base-catalyzed hydrogenation reaction.[5] A six-membered-ring transition structure (Figure 1) that involves the ketone, H_2, and the base catalyst (MOR) has been proposed based on kinetics studies. It has been shown that there is considerable dependence of the reaction rate on the nature of the Group I metal cation (M^+), the alkoxide base ($OR^−$), and the substrate ($XYC=O$). Thus, in the series of Group I alkoxides the rate of the hydrogenation reaction decreases in the order Cs > Rb ≈ K ≫ Na ≫ Li, while aromatic ketones have been found to be more reactive than purely aliphatic substrates.

As a continuation of previous studies,[6] we have been interested in pursuing the fundamentals of transition-metal-free hydrogenation. In the present paper, we employ ab initio molecular orbital theory to study base-catalyzed hydrogenation, in the hope of gaining a better understanding of this subject, and to rationalize the limitations of the catalytic reaction.

(1) For example, see: (a) Rylander, P. N. *Hydrogenation over Platinum Metals*; Academic Press: New York, 1967. (b) Jacobsen, E. N., Pfaltz, A., Yamamoto, H., Eds. *Comprehensive Asymmetric Catalysis*; Springer: Berlin, 1999; Vol. 1. (c) Nishimura, S. *Handbook of Heterogeneous Catalytic Hydrogenation for Organic Synthesis*; Wiley: New York, 2001. (d) Genet, J.-P. *Acc. Chem. Res.* **2003**, *36*, 908.

(2) For general reviews on hydrogenases, see: (a) Albracht, S. P. J. *Biochim. Biophys. Acta* **1994**, *1188*, 167. (b) Ermler, U.; Grabarse, W.; Shima, S.; Goubeaud, M. Thauer, R. K. *Curr. Opin. Struct. Biol.* **1998**, *8*, 749. (c) Evans, D. J.; Pickett, C. J. *Chem. Soc. Rev.* **2003**, *32*, 268.

(3) For example, see: (a) Baltes, J.; Cornils, B.; Frohning, C. D. *Chem. -Ing. -Tech.* **1975**, *47*, 522. (b) Cecchi, G.; Ucciani, E. *Riv. Ital. Sostanze Grasse* **1979**, *56*, 235. (c) Plourde, M.; Belkacemi, K.; Arul, J. *Ind. Eng. Chem. Res.* **2004**, *43*, 2382.

(4) (a) Walling, C.; Bollyky, L. *J. Am. Chem. Soc.* **1961**, *83*, 2968. (b) Walling, C.; Bollyky, L. *J. Am. Chem. Soc.* **1964**, *86*, 3750.

(5) Berkessel, A.; Schubert, T. J. S.; Müller, T. N. *J. Am. Chem. Soc.* **2002**, *124*, 8693.

(6) (a) Scott, A. P.; Golding, B. T.; Radom, L. *New J. Chem.* **1998**, 1171. (b) Senger, S.; Radom, S. *J. Phys. Chem. A* **2000**, *104*, 7375. (c) Senger, S.; Radom, L. *J. Am. Chem. Soc.* **2000**, *122*, 2613. (d) Chan, B.; Radom, L. *Aust. J. Chem.* **2004**, *57*, 659.
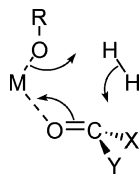
Figure 1. Six-membered-ring transition structure proposed[5] for the base-catalyzed hydrogenation of ketones.

Computational Details

Standard ab initio molecular orbital theory and density functional theory calculations[7] were carried out with the GAUSSIAN 03[8] and MOLPRO 2002[9] programs. Geometries were obtained at the B3-LYP/6-31G(d) level of theory. The intrinsic reaction coordinate (IRC) method was employed to confirm that each transition structure is linked to the appropriate adjacent minima. Improved relative energies were obtained with the high-level G3(MP2)-RAD[10] procedure. Unless otherwise noted, geometrical parameters in the text refer to B3-LYP/6-31G(d) values, while relative energies correspond to the G3(MP2)-RAD values.

In preliminary calculations, carried out to evaluate the effect of diffuse and polarization functions on the optimized structures and the effect of the differences in geometry on the corresponding single-point energies, the geometries and energy profile (0 K) of the reaction $CH_2O + H_2 + NaOCH_3 \rightarrow CH_3OH + NaOCH_3$ obtained at the G3(MP2)-RAD//B3-LYP/6-31G(d) level were compared with those obtained at the G3(MP2)-RAD//B3-LYP/6-31++G(d,p) level. We find that the additional diffuse and polarization functions generally lead to minor changes in geometries and G3(MP2)-RAD relative energies (± 0.02 Å for bond lengths, $\pm 1°$ for bond angles, and ± 2 kJ mol^{-1} for energies). Somewhat larger discrepancies are found for the transition structure (± 0.07 Å for bond lengths, $\pm 4°$ for bond angles, and ± 3 kJ mol^{-1} for energies). Calculations at the G3(MP2)-RAD//B3-LYP/6-31++G(d) and G3(MP2)-RAD//B3-LYP/6-31G(d,p) levels reveal that polarization functions on hydrogen are responsible for the majority of these changes in geometries. These calculations suggest that our use of B3-LYP/6-31G(d) geometries will not lead to significant errors in our calculated energy profiles.

In specific cases involving larger systems, the ONIOM method[11] was employed for single-point energy calculations. We have chosen CCSD(T)/G3MP2Large as our target level in these ONIOM calculations, as this is also the target level for G3(MP2)-RAD. It has been suggested that in ONIOM calculations, with CCSD(T) as the target level, the best choice of low level is MP2.[11f,g] We used either three layers (CCSD(T)/G3MP2Large:MP2/G3MP2Large:MP2/6-31G(d)) or two layers (CCSD(T)/G3MP2Large:MP2/G3MP2Large) in our ONIOM calculations. It has been found that a C−H bond is generally suitable for substitution of a C−C bond.[11f,g] Consequently, in all our ONIOM calculations, hydrogen is used as the link atom whenever a C−C bond is to be replaced.

Unless otherwise noted, zero-point vibrational energies (ZPVEs) and thermal energy corrections (to 483.15 K, 133.27 atm) derived from B3-LYP/6-31G(d) frequencies were incorporated into the G3(MP2)-RAD or ONIOM energies. The temperature and pressure parameters used for the thermal energy corrections were chosen to reflect the experimental reaction conditions (210 °C, 135 bar H_2) detailed in the paper by Berkessel.[5] Literature scaling factors[12] were used in the evaluation of zero-point energies (0.9806), enthalpies (0.9989), and entropies (1.0015) from the B3-LYP/6-31G(d) harmonic vibrational frequencies. The rigid rotor harmonic oscillator approximation[13] was used throughout.

In correlation calculations (MP2, CCSD(T)) that involve potassium and calcium,[14] the correlation space was chosen to include the inner-valence electrons (i.e., 3s and 3p) as well as the valence electrons. This correlation space is denoted relaxed-inner-valence or *riv*.[15] In all other cases, orbitals corresponding to the largest noble gas core were frozen during post-Hartree−Fock calculations.

The necessity of including the 3s and 3p orbitals in the correlation space for Ca- and K-containing molecules has been demonstrated previously.[15] For instance, heats of formation obtained with the G2 method but without relaxation of the inner-valence electrons are in poor agreement with experimental results for KOH ($+160$ kJ mol^{-1} discrepancy) and Ca(OH)$_2$ ($+86$ kJ mol^{-1} discrepancy), respectively, while G2(*riv*) gives much smaller discrepancies ($+9$ kJ mol^{-1} for KOH and $+21$ kJ mol^{-1} Ca(OH)$_2$).[15b] In these cases, the mixing of the 3s and 3p orbitals of the metal with valence orbitals on oxygen is the key reason that the exclusion of the former is inappropriate and can lead to poor results.

Solvent effects were evaluated at the B3-LYP/6-31G(d) level using the integral equation formalism polarizable continuum model (IEF-PCM)[16] through calculations on the optimized gas-phase structures. Unless noted otherwise, methanol was used as the solvent for the IEF-PCM calculations. For comparison, solvation studies on selected systems were also conducted with the self-consistent isodensity

(7) For example, see: (a) Hehre, W. J.; Radom, L.; Schleyer, P. v. P.; Pople, J. A. *Ab Initio Molecular Orbital Theory*; Wiley: New York, 1986. (b) Jensen, F. *Introduction to Computational Chemistry*; Wiley: Chichester, 1998. (c) Koch, W.; Holthausen, M. C. *A Chemist's Guide to Density Functional Theory*, 2nd ed.; Wiley: New York, 2001.

(8) Frisch, M. J.; Trucks, G. W.; Schlegel, H. B.; Scuseria, G. E.; Robb, M. A.; Cheeseman, J. R.; Montgomery, J. A., Jr.; Vreven, T.; Kudin, K. N.; Burant, J. C.; Millam, J. M.; Iyengar, S. S.; Tomasi, J.; Barone, V.; Mennucci, B.; Cossi, M.; Scalmani, G.; Rega, N.; Petersson, G. A.; Nakatsuji, H.; Hada, M.; Ehara, M.; Toyota, K.; Fukuda, R.; Hasegawa, J.; Ishida, M.; Nakajima, T.; Honda, Y.; Kitao, O.; Nakai, H.; Klene, M.; Li, X.; Knox, J. E.; Hratchian, H. P.; Cross, J. B.; Adamo, C.; Jaramillo, J.; Gomperts, R.; Stratmann, R. E.; Yazyev, O.; Austin, A. J.; Cammi, R.; Pomelli, C.; Ochterski, J. W.; Ayala, P. Y.; Morokuma, K.; Voth, G. A.; Salvador, P.; Dannenberg, J. J.; Zakrzewski, V. G.; Dapprich, S.; Daniels, A. D.; Strain, M. C.; Farkas, O.; Malick, D. K.; Rabuck, A. D.; Raghavachari, K.; Foresman, J. B.; Ortiz, J. V.; Cui, Q.; Baboul, A. G.; Clifford, S.; Cioslowski, J.; Stefanov, B. B.; Liu, G.; Liashenko, A.; Piskorz, P.; Komaromi, I.; Martin, R. L.; Fox, D. J.; Keith, T.; Al-Laham, M. A.; Peng, C. Y.; Nanayakkara, A.; Challacombe, M.; Gill, P. M. W.; Johnson, B.; Chen, W.; Wong, M. W.; Gonzalez, C.; Pople, J. A. *Gaussian 03*, revision B.03; Gaussian, Inc.: Pittsburgh, PA, 2003.

(9) MOLPRO, a package of ab initio programs designed by H.-J. Werner and P. J. Knowles, version 2002.1. R. D. Amos, A. Bernhardsson, A. Berning, P. Celani, D. L. Cooper, M. J. O. Deegan, A. J. Dobbyn, F. Eckert, C. Hampel, G. Hetzer, P. J. Knowles, T. Korona, R. Lindh, A. W. Lloyd, S. J. McNicholas, F. R. Manby, W. Meyer, M. E. Mura, A. Nicklass, P. Palmieri, R. Pitzer, G. Rauhut, M. Schütz, U. Schumann, H. Stoll, A. J. Stone, R. Tarroni, T. Thorsteinsson, and H.-J. Werner.

(10) (a) Henry, D. J.; Sullivan, M. B.; Radom, L. *J. Chem. Phys.* **2001**, *118*, 4849. (b) Henry, D. J.; Parkinson, C. J.; Mayer, P. M.; Radom, L. *J. Phys. Chem. A* **2001**, *105*, 6750. (c) Henry, D. J.; Sullivan, M. B.; Radom, L. *J. Chem. Phys.* **2003**, *118*, 4849.

(11) (a) Maseras, F.; Morokuma, K. *J. Comput. Chem.* **1995**, *16*, 1170. (b) Humbel, S.; Sieber, S.; Morokuma, K. *J. Chem. Phys.* **1996**, *105*, 1959. (c) Matsubara, T.; Sieber, S.; Morokuma, K. *Int. J. Quantum Chem.* **1996**, *60*, 1101. (d) Svensson, M.; Humbel, S.; Froese, R. D. J.; Matsubara, T.; Sieber, S.; Morokuma, K. *J. Phys. Chem.* **1996**, *100*, 19357. (e) Svensson, M.; Humbel, S.; Morokuma, K. *J. Chem. Phys.* **1996**, *105*, 3654. (f) Dapprich, S.; Komáromi, I.; Byun, K. S.; Morokuma, K.; Frisch, M. J. *THEOCHEM* **1999**, *462*, 1. (g) Vreven, T.; Morokuma, K. *J. Comput. Chem.* **2000**, *21*, 1419.

(12) Scott, A. P.; Radom, L. *J. Phys. Chem.* **1996**, *100*, 16502.

(13) Bloch S. C. *Introduction to Classical and Quantum Harmonic Oscillators*; Wiley: Canada, 1997.

(14) The G3MP2Large basis set for potassium and calcium used in G3(MP2)-RAD calculations can be downloaded from the website http://chemistry-.anl.gov/compmat/g3theory.htm.

(15) (a) Blaudeau, J.-P.; McGrath, M. P.; Curtiss, L. A.; Radom, L. *J. Chem. Phys.* **1997**, *107*, 5016. (b) Schulz, A.; Smith, B. J.; Radom, L. *J. Phys. Chem. A* **1999**, 103, 7522. (c) Curtiss, L. A.; Redfern, P. C.; Rassolov, V.; Kedziora, G.; Pople, J. A. *J. Chem. Phys.* **2001**, *114*, 9287. (d) Sullivan, M. B.; Iron, M. A.; Redfern, P. C.; Martin, J. M. L.; Curtiss, L. A.; Radom, L. *J. Phys. Chem. A* **2003**, *107*, 5617.

(16) (a) Cancès, M. T.; Mennucci, B.; Tomasi, J. *J. Chem. Phys.* **1997**, *107*, 3032. (b) Mennucci B.; Tomasi, J. *J. Chem. Phys.* **1997**, *106*, 5151. (c) Mennucci, B.; Cancès, E., Tomasi, J. *J. Phys. Chem. B* **1997**, *101*, 10506. (d) Tomasi, J.; Mennucci, B.; Cancès, E. *THEOCHEM* **1999**, *464*, 211.
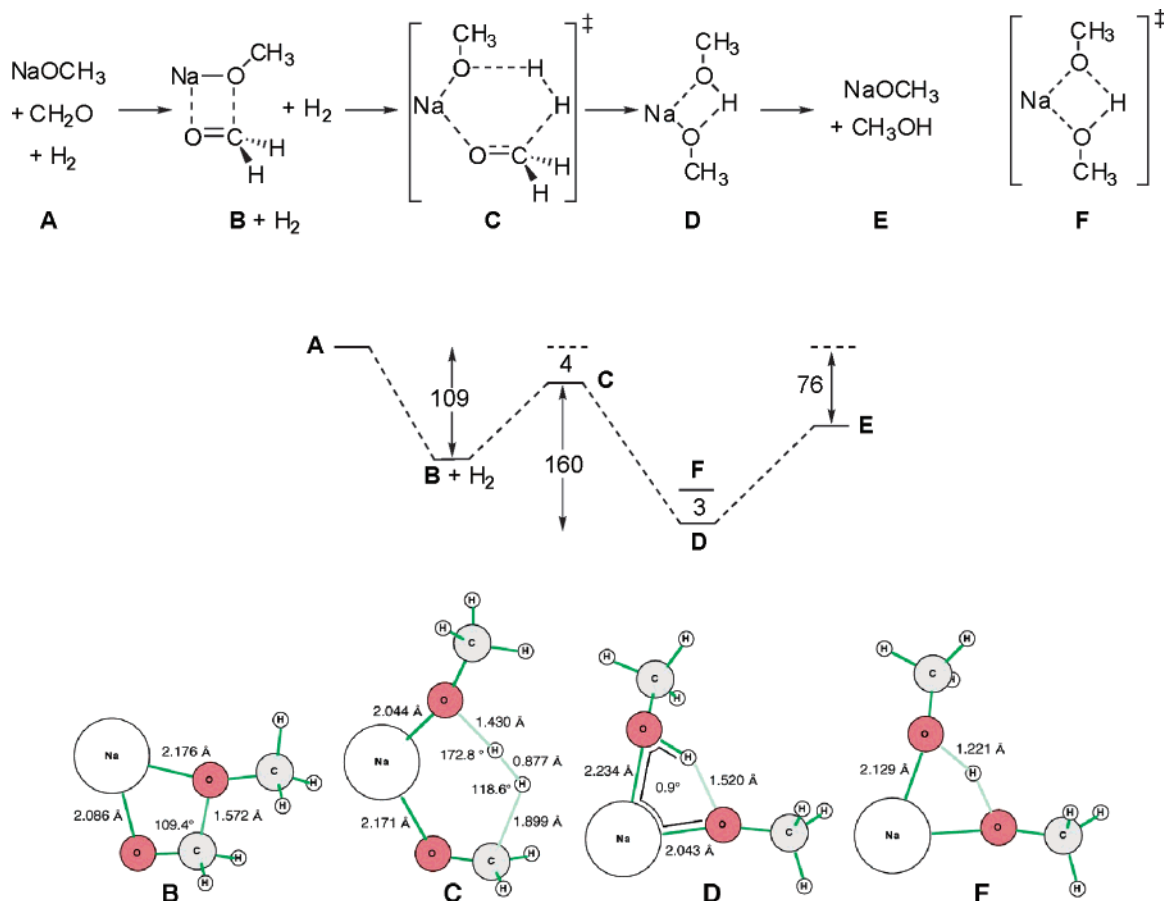
Figure 2. Hydrogenation of formaldehyde catalyzed by NaOCH$_3$. Energy profile at 0 K (kJ mol^{-1}) and selected optimized structures.

polarizable continuum model (SCI-PCM).[17] We find that the two models give comparable solvation energies.

Hydrogenation of Formaldehyde Catalyzed by Sodium Methoxide

A. Energy Profile at 0 K. We have chosen the sodium-methoxide-catalyzed hydrogenation reaction of formaldehyde as a simple model to assess the energy profile of general base-catalyzed hydrogenations. The calculated G3(MP2)-RAD profile of the reaction at 0 K (i.e., including zero-point vibrational energy), together with optimized geometries of selected species along the reaction pathway, is shown in Figure 2.

Sodium methoxide forms a strong adduct with formaldehyde (**B**), with a ΔH of -109 kJ mol^{-1}. The distance between methoxy oxygen and the formaldehyde carbon is 1.572 Å, which is somewhat longer than the bond length of a typical C—O bond (e.g., 1.419 Å in CH$_3$—OH). The $\angle$O—C—O bond angle of 109.4° is almost identical to the tetrahedral angle (109.5°). The sodium atom is strongly associated with both oxygen atoms, with Na—O bond lengths to the methoxy and the formaldehyde oxygen of 2.176 and 2.086 Å, respectively, slighter longer than that in sodium methoxide (1.931 Å). In the transition structure (**C**), the sodium atom retains strong interactions with both oxygen atoms. The Na—OCH$_3$ and Na—OCH$_2$ distances are now 2.044 and 2.171 Å, respectively. There is an almost linear

arrangement between the methoxy oxygen and H$_2$, with an $\angle$O—H—H angle of 172.8°, while the H—H—C linkage is highly angular with an $\angle$H—H—C angle of 118.6°. Such a near-linear arrangement for the proton acceptor and angular arrangement for the hydride acceptor in the heterolytic cleavage of H$_2$ have been noted previously.[6a,18] The transition structure **C** lies 105 kJ mol^{-1} above the NaOCH$_3$—CH$_2$O adduct (**B**) plus H$_2$. However, the hydrogenation reaction has no overall barrier ($\Delta E_{C-A} = -4$ kJ mol^{-1}). After traversing the transition structure, a strong complex (**D**) between the eventual products, sodium methoxide and methanol (**E**), is formed. Once again, the sodium atom in **D** is strongly associated with both oxygen atoms, with Na—O distances to the methanol and the methoxy oxygen atoms of 2.234 and 2.043 Å, respectively. The sodium atom, the two oxygen atoms, and the hydroxy proton of methanol practically lie in the same plane ($\angle$O—Na—O—H dihedral angle = 0.9°). The hydroxy proton is strongly hydrogen-bonded to the oxygen of the newly formed methoxide (H$\cdots$O = 1.520 Å). A transition structure (**F**) corresponding to the proton exchange between the two methoxy units, which lies only 3 kJ mol^{-1} above complex **D**, has also been located. Isolated products **E** lie 88 kJ mol^{-1} higher in energy than the complex **D**, and the ΔH of the overall reaction is -76 kJ mol^{-1}. Interestingly, this qualitative energy profile is similar to that found for gas-phase S$_N$2 reactions,[19] which are also described by two-well energy profiles.

(17) (a) Wiberg, K. B.; Keith, T. A.; Frisch, M. J.; Murcko, M. *J. Phys. Chem.* **1995**, *99*, 7702. (b) Foresman, J. B.; Keith, T. A.; Wiberg, K. B.; Snoonian, J.; Frisch, M. J. *J. Phys. Chem.* **1996**, *100*, 16098.

(18) For example, see: (a) Orlova, G.; Scheiner, S.; Kar, T. *J. Phys. Chem. A* **1999**, *103*, 514. (b) Yu, Z.; Wittbrodt, J. M.; Xia, A.; Heeg, M. J.; Schlegel, H. B.; Winter, C. H. *Organometallics* **2001**, *20*, 4301.
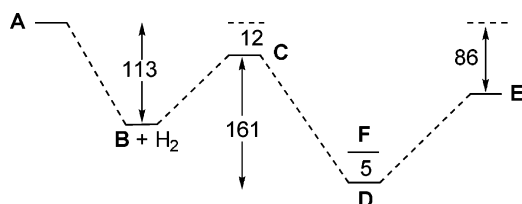
Figure 3. Enthalpy profile (ΔH, kJ mol^{-1}) for the NaOCH$_3$-catalyzed hydrogenation of formaldehyde at 483.15 K under 133.27 atm.
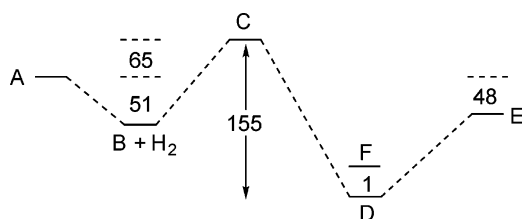

Figure 4. Gibbs free energy profile (ΔG, kJ mol^{-1}) for the NaOCH$_3$-catalyzed hydrogenation of formaldehyde at 483.15 K under 133.27 atm.

B. Enthalpy and Free Energy Profiles at 483.15 K. To evaluate the effect of thermal energies and entropies on the reaction, appropriate corrections were applied to the 0 K energies. A temperature of 483.15 K and a pressure of 133.27 atm were employed, in keeping with the experimental conditions.[5] The enthalpy (ΔH) and free energy (ΔG) profiles are shown in Figures 3 and 4, respectively. We note that at 0 K, $\Delta E = \Delta H = \Delta G$ and so the energy profile in Figure 2 corresponds to any of these quantities at 0 K.

While the enthalpy profile at 483.15 K (Figure 3) is fairly similar to the energy profile at 0 K, the free energy profile at 483.15 K (Figure 4) is substantially different. In particular, the formation of adduct **B** is now exothermic by only 51 kJ mol^{-1}, less than half of the binding energy at 0 K. Furthermore, the hydrogenation reaction now has an overall free energy barrier of 65 kJ mol^{-1}. The complex **D** lies 155 kJ mol^{-1} lower in energy than the transition structure, while transition structure **F** lies 1 kJ mol^{-1} above the base–methanol complex. The overall ΔG for the reaction is −48 kJ mol^{-1}, which is 28 kJ mol^{-1} less than the exothermicity at 0 K.

Our calculated free energy profile (Figure 4) indicates that entropy has a substantial effect on the hydrogenation reaction. In this case, for instance, the inclusion of $\Delta S^{\ddagger}$ leads to a $\Delta G^{\ddagger}$ that is 77 kJ mol^{-1} more positive than the corresponding $\Delta H^{\ddagger}$. It has been previously suggested that in the base-catalyzed hydrogenation, the assembling of the highly ordered transition structure (an entropic effect) is the limiting factor in the reaction.[5] The theoretical results presented here are consistent with this hypothesis.

C. Free Energy Profile in Solution. The effect of solvent on the reaction profile was evaluated through calculations of the solvation energy, i.e., the difference between the solution-phase free energy and the gas-phase free energy ($\Delta G_{solv} = G_{soln} - G_{gas}$). It is important to note that the IEF-PCM method employed here represents the solvent as a continuum of uniform dielectric constant. This only represents part of the effect of the solvent, in that specific interactions such as hydrogen
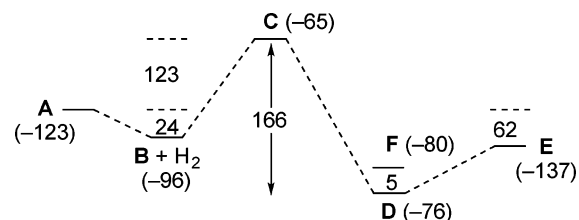

Figure 5. Gibbs free energy profile (kJ mol^{-1}) for the NaOCH$_3$-catalyzed hydrogenation of formaldehyde in methanol at 483.15 K under 133.27 atm. Solvation energies (kJ mol^{-1}) are given in parentheses.

bonding are not explicitly included. Hence, the results should be interpreted largely in terms of qualitative trends rather than as an exact quantitative treatment of solvent effects. The solution free energy profile (including the solvation energies for all of the species) is shown in Figure 5.

At all stages of the reaction, solvation leads to a large stabilization. The value of ΔG_{solv} ranges from −65 kJ mol^{-1} for transition structure **C** to −137 kJ mol^{-1} for products **E**. The wide range of solvation stabilization gives rise to a significantly different free energy profile to that calculated for the gas phase (Figure 4). Noticeably, the adduct **B** is now only 24 kJ mol^{-1} lower in energy than the isolated components. The overall barrier is 123 kJ mol^{-1}, while the barrier calculated from **B** + H$_2$ is 147 kJ mol^{-1}, which is substantially higher than the corresponding gas-phase value (116 kJ mol^{-1}). The overall free energy change for the reaction is −62 kJ mol^{-1}, which is somewhat larger than the gas-phase value.

The difference in gas-phase and solution-phase energy profiles can be explained by the difference in solvation energy at different points along the reaction coordinate. Thus, compared with separated reactants (**A**), the charge in the reactant complex **B** is more delocalized. Consequently, the polar solvent interacts with the complex less strongly than with the isolated species, resulting in a lower solvation energy. In the transition structure **C**, even more charge delocalization would be expected as a result of the more compact structure, resulting in an even lower solvation energy than that in the adduct. The energy profile of Figure 5 again parallels the behavior found for solution-phase S$_N$2 reactions, in which the two energy wells become much shallower, or disappear completely, as compared with the gas-phase profiles.[19,20]

D. Substitution of Hydrogen by Deuterium. We have investigated the effect on the free energy barrier of replacing H by D (H$_2$/HD/D$_2$) using appropriately modified vibrational frequencies in the calculation of ZPVE and thermal corrections. In the case of HD, scenarios where either H or D acts as the hydride/deuteride were both investigated. Our results indicate that substituting D$_2$ or HD for H$_2$ leads to only a slight increase in barrier ($\leq$+3 kJ mol^{-1}). This is consistent with the experimental observation that base-catalyzed hydrogenation does not show a significant kinetic isotopic (H$_2$/HD) effect.[5] However, the small effect on the barrier does not explain the experimental observation of a low rate of reaction for D$_2$. In addition, we find that tunneling corrections are small at the elevated

(19) For recent reviews on gas-phase S$_N$2 reactions, see: (a) Chabinyc, M. L.; Craig, S. L.; Regan, C. K.; Brauman, J. I. *Science* **1998**, *279*, 20. (b) Gronert, S. *Chem. Rev.* **2001**, *101*, 329. (c) Laerdahl, J. K.; Uggerud, E. *Int. J. Mass Spectrom.* **2002**, *214*, 277. See also: (d) Shaik, S. S.; Schlegel, H. B.; Wolfe, S. *Theoretical aspects of physical organic chemistry: the S$_N$2 mechanism*; Wiley: New York, 1992.

(20) For example, see: (a) Streitwieser, A. *Solvolytic Displacement Reactions*; McGraw-Hill: New York, 1962. (b) Ingold, C. K. *Structure and Mechanism in Organic Chemistry*, 2nd ed.; Cornell University Press: New York, 1969. (c) Olmstead, W. N.; Brauman, J. I. *J. Am. Chem. Soc.* **1977**, *99*, 4219. (d) Tucker, S. C.; Truhlar, D. G. *Chem. Phys. Lett.* **1989**, *157*, 164. (e) Regan, C. K.; Craig, S. L. Brauman, J. I. *Science* **2002**, *295*, 2245.

Table 1. Gibbs Free Energies (ΔG, kJ mol^{-1})^a for the MOCH$_3$-Catalyzed Hydrogenation of Formaldehyde

	reaction	M	B + H$_2$	C^b	D	E	$\Delta G^{\ddagger}_{cent}$ ^{c}
gas phase	1	Li	−45	64	−82	−48	109
	2	Na	−51	65	−90	−48	116
	3	K	−47	69	−95	−48	116
solution phase	1	Li	−20	131	−26	−62	151
	2	Na	−24	123	−43	−62	147
	3	K	−33	107	−63	−62	140

^{a} Calculated relative to the reactants **A**. ^{b} By definition, the relative energy of **C**, ΔG_{C-A}, is also the overall barrier for the reaction ($\Delta G^{\ddagger}_{ovr}$). ^{c} The central barrier is the difference between the free energy of **C** and that of **B** + H$_2$.

temperatures used in the experimental work. So the reason for the unusual H$_2$/D$_2$ difference remains unclear.

Substituent and Solvent Effects: General Considerations

With this basic knowledge of the reaction profile established, we now proceed to investigate the effect of the metal, the base, the substrate, and the solvent on the energy profile. From this point on, the relative energies refer to ΔG values at 483.15 K with a pressure of 133.27 atm. The $\Delta G^{\ddagger}$ values are referred to in the text as barriers for simplicity. Both gas-phase as well as solution-phase relative energies will be discussed. For a reaction with a double-well energy profile, the gas-phase reaction rate depends on a number of factors, including temperature and pressure.[21] At the low-pressure limit with minimal deactivation via collisions, the effective barrier normally corresponds to the energy relative to isolated reactants, i.e., the free energy of **C** relative to **A** (overall barrier, $\Delta G^{\ddagger}_{ovr}$). At the high pressure limit, the effective barrier corresponds to the energy difference between the transition structure and the energy well that immediately precedes it on the reaction pathway, i.e., the free energy of **C** relative to **B** + H$_2$ (central barrier, $\Delta G^{\ddagger}_{cent}$). We will therefore discuss the central, as well as the overall, energy barriers for gas-phase reactions. In solution, the conditions are virtually equivalent to the high-pressure limit with very effective collisional deactivation. Thus, the reaction rate is largely determined by the central barrier, i.e., the energy measured from the adjacent energy well. In a small number of cases, the calculated free energy of the reactant complex is higher than that of the isolated reactants. In these cases, we have taken the barriers to correspond to the energy difference between the transition structure and that of the isolated reactants, i.e., $\Delta G^{\ddagger}_{ovr}$.

Effect of Metal

A. Group I Metals: Li, Na, and K. To explore the effects of varying the metal ion (M), hydrogenation of formaldehyde catalyzed by various main-group methoxides has been investigated. We begin with the reactions of Group I methoxides

(M = Li, Na, and K). The optimized structures with Li and K are very similar to those with Na (Figure 2). The gas-phase and solution-phase energy profiles of these Group-I-methoxide-catalyzed hydrogenation reactions are summarized in Table 1.

The gas-phase catalytic activity for the Group I methoxides, although varying only very slightly with the metal, is in the order Li > Na > K. This is in contrast to the experimental trend, the catalytic activity in the hydrogenation of benzophenone among Group I benzhydrolates increasing in the order Li < Na < K.[5] However, after the inclusion of solvation energies, the experimental ordering is obtained (Table 1).

The reversal of the trends found between gas-phase and solution-phase reactivities can be rationalized in terms of the charge density of Group I cations and their relative degree of solvation. Thus, Li$^+$ is a small cation with a high charge density. In the gas phase, it strongly withdraws electron density from formaldehyde and, hence, activates it toward attack by the hydride ion formed from heterolytic cleavage of H$_2$. On the other hand, the larger K$^+$ has a lower charge density, and it is less effective in activating formaldehyde toward nucleophilic attack. In solution, the smaller Li$^+$ receives considerably higher stabilization from solvation than the larger K$^+$. In addition, as discussed earlier, solvent stabilization is larger in the separated species **A** than in the transition structure **C**. The net result is that the solvation-induced increase in the barrier is more pronounced for Li than for K. In this case, solvent effects dominate the solution-phase reaction, and hence opposite trends are observed in the gas phase and in solution. Interestingly, these opposite reactivity trends in gas and solution phases are analogous to the trends in halide reactivity in S$_N$2 reactions. Thus, in the gas-phase F$^-$ is the strongest nucleophile,[20c,22] while in a polar protic solvent the most nucleophilic ion is I$^-$.[23]

B. Group II and III Metals: Be, Mg, Ca, B, and Al. Hydrogenation reactions catalyzed by several Group II and Group III methoxides have also been investigated. Selected optimized structures in the Mg(OCH$_3$)$_2$-catalyzed reaction are

(21) For example, see: (a) Dean, A. M. *J. Phys. Chem.* **1985**, *89*, 4600. (b) Oref, I. *J. Phys. Chem.* **1989**, *93*, 3465. (c) Fahr, A.; Laufer, A. H.; Tardy, D. C. *J. Phys. Chem. A* **1999**, *103*, 8433. (d) Golden, D. M.; Barker, J. R.; Lohr, L. L. *J. Phys. Chem. A* **2003**, *107*, 11057. (e) de Persis, S.; Dollet, A.; Teyssandier, F. *J. Chem. Educ.* **2004**, *81*, 832.

(22) For example, see: (a) Brauman, J. I.; Olmstead, W. N.; Lieder, C. A. *J. Am. Chem. Soc.* **1974**, *96*, 4030. (b) Tanaka, K.; Mackay, G. I.; Payzant, J. D.; Bohme, D. K. *Can. J. Chem.* **1976**, *54*, 1643.

(23) For example, see: (a) McCleary, H. R.; Hammett, L. P. *J. Am. Chem. Soc.* **1941**, *63*, 2254. (b) Pearson, R. G.; Sobel, H.; Songstad, J. *J. Am. Chem. Soc.* **1968**, *90*, 319. (c) Parker, A. J. *Chem. Rev.* **1969**, *69*, 1.
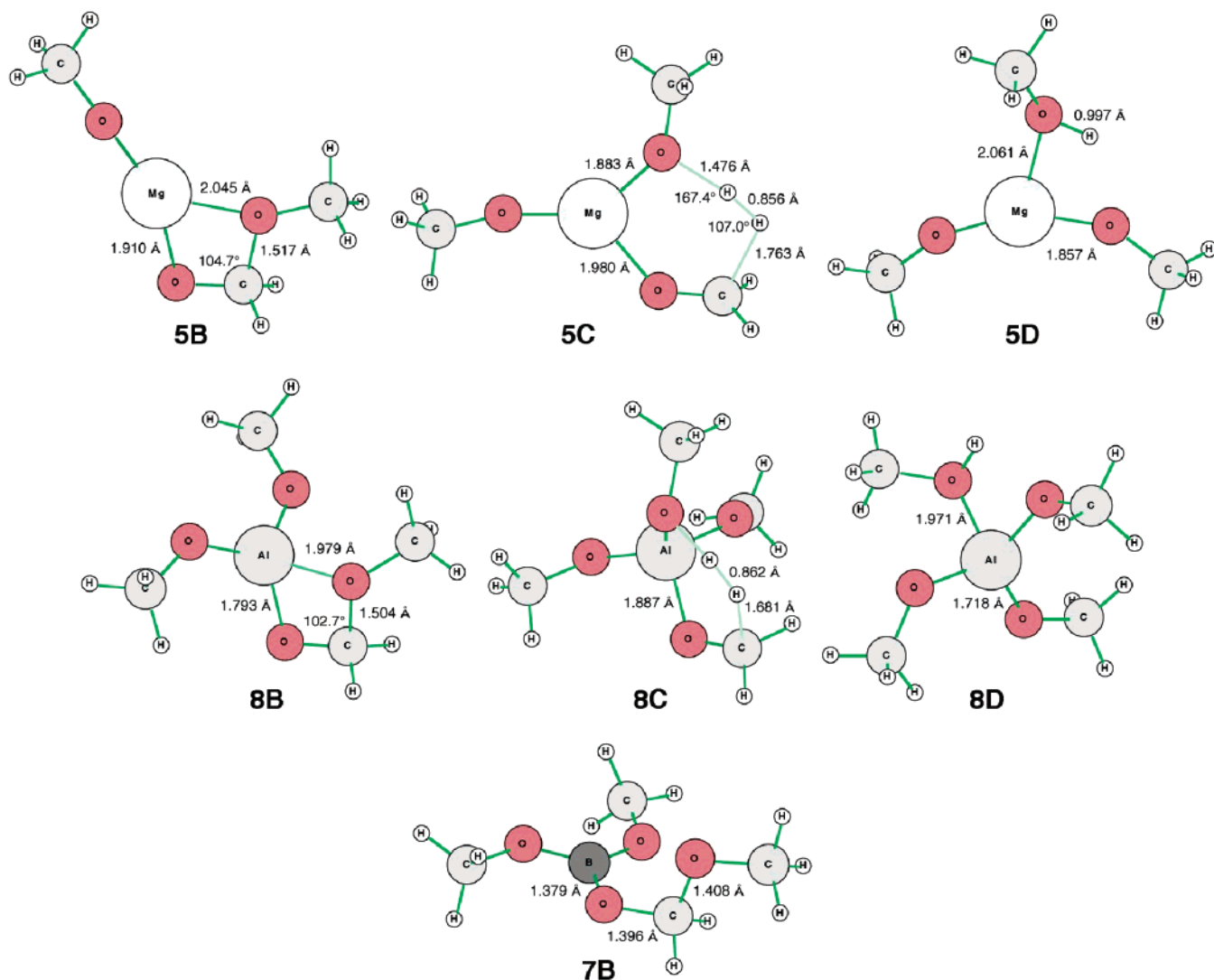
Figure 6. Selected optimized structures involved in the Group II/III methoxide-catalyzed hydrogenation of formaldehyde: (**5B−D**) Mg; (**8B−D**) Al; and (**7B**) B.

shown in Figure 6 as a representative example for reactions with Group II methoxides. Also included are selected optimized structures for the reactions involving Group III methoxides. The Group II structures are similar to their corresponding Group I counterparts. However, some of the Group III species have significantly different structures to both their Group I and Group II analogues. Thus, in the transition structures (**C**) with a Group I or a Group II metal, the dihedral angle ∠M−O−C−H to the formaldehyde hydrogen is almost 90°. On the other hand, the corresponding dihedral angle in the Group III transition structures is approximately 45°. The metals of these Group III methoxides might interact strongly with the lone pair of formaldehyde, which in turn leads to the different directional properties compared with the Group I and Group II methoxides. Furthermore, several attempts at locating a complex between $B(OCH_3)_3$ and formaldehyde led to the structure (**7B**) shown in Figure 6. Presumably, the π-electron donation from the oxygen lone pairs of the three methoxy groups practically fills the vacant p orbital on the boron, thereby prohibiting the formation of a fourth B−O bond. This type of back-bonding between boron and small π-donor substituents has been well

documented.[24] For instance, it has been used to explain the increases in Lewis acidities of boron trihalides down the group $BF_3 < BCl_3 < BBr_3$,[24] the opposite of what would be expected from the electronegativities of the halogens.

The energy profiles of the Group II- and Group-III-methoxide-catalyzed reactions are summarized in Table 2. The lower overall gas-phase barriers for Mg and Ca than for the corresponding Group I metals (Table 1) are consistent with their higher formal charge and, hence, stronger interaction with formaldehyde. On the other hand, the $Be(OCH_3)_2$-catalyzed reaction has a higher barrier than that of $LiOCH_3$. This can be attributed to the high covalency of the Be−O bonds in $Be(OCH_3)_2$, which leads to a low partial charge on beryllium and, hence, a relatively low catalytic activity. It is well documented that beryllium compounds are highly covalent.[25] For instance, beryllium chloride has a substantially lower melting point of 399 °C, as compared with 714 °C and 772 °C for $MgCl_2$ and $CaCl_2$, respectively.[26]

(24) For example, see: (a) Brown, H. C.; Holmes, R. R. *J. Am. Chem. Soc.* **1956**, *78*, 2173. (b) Shriver, D. F.; Swanson, B. *Inorg. Chem.* **1971**, *10*, 1354. (c) Pearson, R. G. *Inorg. Chem.* **1988**, *27*, 734. (d) Liebman, J. F. *Struct. Chem.* **1990**, *1*, 395. (e) Sreekanth, C. S.; Mok, L. Y.; Huang, H. H.; Tan, K. L. *J. Electron Spectrosc. Relat. Phenom.* **1992**, *58*, 129.

A R T I C L E S

Table 2. Gibbs Free Energies (ΔG, kJ mol^{-1})^a for the $M(OCH_3)_n$-Catalyzed^b Hydrogenation of Formaldehyde
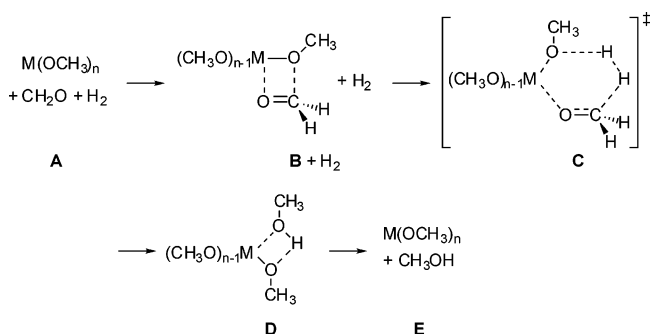
	reaction	M	B + H$_2$	C^c	D	E	$\Delta G^{\ddagger}_{cent}$ ^{d}
gas phase	**4**	Be	−28	101	−101	−48	129
	5	Mg	−64	56	−108	−48	120
	6	Ca	−73	51	−115	−48	124
	7	B	23	255	16	−48	255^e
	8	Al	−31	100	−91	−48	131
solution phase	**4**	Be	−34	96	−119	−62	130
	5	Mg	−23	119	−35	−62	142
	6	Ca	−31	129	−44	−62	160
	7	B	23	246	6	−62	246^e
	8	Al	−38	94	−101	−62	132

^{a} Calculated relative to the reactants **A**. ^{b} $n = 2$ for Be, Mg, and Ca; $n = 3$ for B and Al. ^{c} By definition, the relative energy of **C** (ΔG_{C-A}) is also the overall barrier of the reaction ($\Delta G^{\ddagger}_{ovr}$). ^{d} The central barrier is the difference between the free energy of **C** and that of **B** + H$_2$. ^{e} Because **B** + H$_2$ lies higher in energy than **A**, the central barrier is taken as ΔG_{C-A} in this case.

It is interesting to see that, despite the large variation in overall barriers, the central barriers fall into a small range. Presumably, the metal methoxide/formaldehyde interactions are comparable in the adduct and in the transition structure, leading to the small variation in the central barriers. This is again similar to the behavior in gas-phase S$_N$2 reactions, where the central barriers of identity exchange reactions of various *para*-substituted-benzyl chlorides with Cl$^-$ lie in a narrow range, while their overall barriers vary widely.[27]

Both Group III methoxides lead to higher overall barriers than those of corresponding Group I methoxides (Table 1), especially in the case of B(OCH$_3$)$_3$, with a remarkably high value of 255 kJ mol^{-1}. Presumably, this can also be partly attributed to the covalency of Group III compounds. However, the much higher barrier for the B(OCH$_3$)$_3$ reaction might also be indicating the presence of other unfavorable factors. In particular, π-electron donation from the methoxy groups to the boron dramatically weakens its interaction with formaldehyde, leading to the much higher barrier. In solution, the barriers for the reactions of Group II and aluminum methoxides are comparable to those of Group I methoxides, while the barrier for the B(OCH$_3$)$_3$-catalyzed reaction remains considerably higher.

An interesting feature emerges when a comparison is made between Group II methoxides and Group I methoxides. The

barriers within the Group-I-methoxide-catalyzed reactions increase down the group for the gas-phase reactions but decrease down the group in solution (Table 1). On the other hand, the Group II catalysts give rise to opposite trends, both in the gas phase and in solution; i.e., the barriers decrease down the group in the gas phase but increase down the group in solution. Furthermore, in the gas phase, the barriers for Group III methoxides also decrease down the group (Table 2).

Unlike Group I metals, which form highly ionic compounds, the covalency within Group II and within Group III compounds varies widely. For Group II metals, the ionic character increases down the group, and a larger charge on the metal cation would be expected, resulting in a decrease in barrier down the group. In a polar solvent, however, a more ionic Group II cation would be expected to experience larger solvation, leading to a more severely lowered catalytic activity. At the covalent extreme, the gas-phase and solution-phase energy profiles of the Be(OCH$_3$)$_2$ reaction are remarkably similar, indicating that solvation has a very minor effect. Solvation also has little effect on the energy profile of both of the Group III methoxides, leading to the same trends in the gas phase and in solution.

Effect of the Anionic Base

To elucidate the effect of the anionic base on the catalytic activity, the energy profiles for hydrogenation of formaldehyde catalyzed by lithium, sodium, and potassium *tert*-butoxides and benzyloxides were examined. Selected optimized structures for the reactions with Na as the counterion are presented in Figure 7 as representative examples.

While the optimized structures for the *tert*-butoxide reactions generally resemble those of the corresponding methoxide analogues, the structures for species involved in the benzyloxide reactions show some interesting differences. For the catalysts MOCH$_2$Ph, the adducts **B**, and the complexes **D**, there is an "open" form and a "closed" form, the latter having the metal in close proximity to the benzene ring. Several attempts at optimizations of the transition structure **C** from different starting geometries all led to the closed form. In addition, optimizing the open form of the transition structure with the Onsager solvation model also led to the closed form. Nevertheless, it is possible that the open form can be located as a minimum by the means of optimizing with a more sophisticated solvent model (e.g., PCM) or by the inclusion of explicit solvent molecules. Metal cation/π-complex interaction similar to that in the closed forms has been well documented.[28] It has also been suggested that, in the base-catalyzed hydrogenation of aromatic ketones, π-complexation to Group I cations might be important in the catalysis.[5] The reaction profiles for the *tert*-butoxide- and benzyloxide-catalyzed hydrogenations are summarized in Table 3.

The trends in catalytic activity of the *tert*-butoxides parallel those of Group I methoxides (Table 1), both in the gas phase and in solution. Moreover, these solution-phase barriers are comparable to those of Group I-methoxide-catalyzed reactions, indicating that the catalytic activity of the base is relatively insensitive to the size of the alkoxide.

(25) (a) Everest, D. A. In *Comprehensive Inorganic Chemistry*; Bailar, J. C., Jr., Eméléus, H. J., Nyholm, R., Trotman-Dickenson, A. F., Eds.; Pergamon: Oxford, 1973; Vol. 1. (b) Greenwood, N. N.; Earnshaw, A. *Chemistry of the Elements*, 2nd ed.; Butterworth: Boston, 1997. (c) Cotton, F. A.; Wilkinson, G.; Murillo, C. A.; Bochmann, M. *Advanced Inorganic Chemistry*, 6th ed.; Wiley: New York, 1999.
(26) Aldrich Chemical Co. *Aldrich Catalog/Handbook of Fine Chemicals*, 2000−2001 ed.; Aldrich: Milwaukee, WI, 2000.
(27) Wladkowski, B. D.; Wilbur, J. L.; Brauman, J. I. *J. Am. Chem. Soc.* **1994**, *116*, 2471.

(28) For example, see: (a) Ma, J. C.; Dougherty, D. A. *Chem. Rev.* **1997**, *97*, 1303. (b) Fuji, T. *Mass Spectrom. Rev.* **2000**, *19*, 11. (c) Rodgers, M. T.; Armentrout, P. B. *Mass Spectrom. Rev.* **2000**, *19*, 215. (d) Amunugama, R.; Rodgers, M. T. *Int. J. Mass Spectrom.* **2003**, *222*, 431.
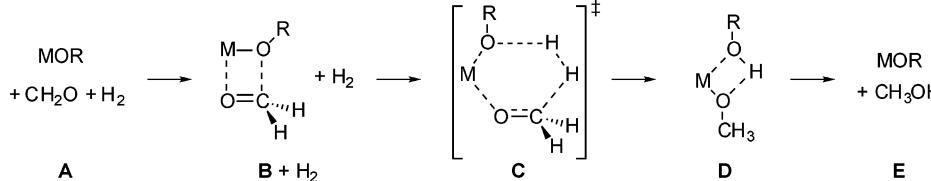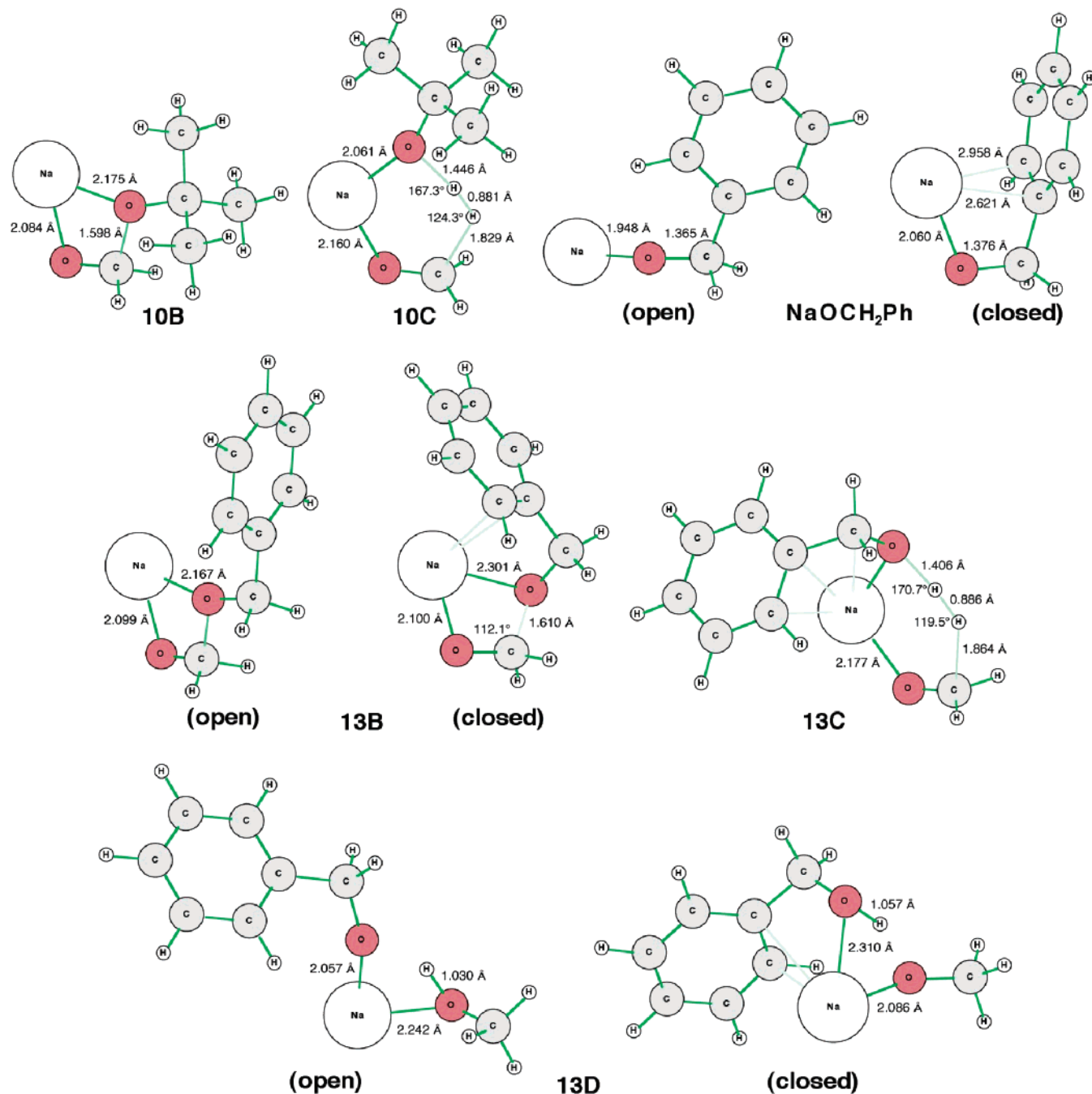
Figure 7. Selected optimized structures involved in the hydrogenation of formaldehyde catalyzed by Na−O−*t*-Bu (**10B,C**), and Na−OCH₂Ph (**NaOCH₂Ph**, plus **13B−D**).

For the Group-I-benzyloxide-catalyzed reactions, in the gas phase, the open form is the more stable conformation for most species. This is somewhat surprising, as it is well-known that Group I cations form stable π-complexes with benzene derivatives.[28] Presumably, the formation of the closed conformer also introduces unfavorable factors which, in most cases, appear to be large enough to offset the attractive π-interactions. The overall barriers for the benzyloxide reactions are somewhat higher than those for the corresponding methoxides, while the central barriers are comparable.

In solution, the open conformers of **A**, **B**, **D**, and **E** are all lower in energy than the corresponding closed forms, but for the transition structure **C**, only a closed form is found in our calculations, as noted above. The energy differences between the closed and open forms are generally larger in solution than in the gas phase. Presumably, the metal cations in open conformers are more exposed and hence are better solvated than those in the closed forms. This would also decrease the extent of interaction with the π-systems. The solution-phase barriers are somewhat higher than values for the corresponding methoxides (Table 1) and *tert*-butoxides (Table 3). The difference in reactivity is most pronounced for Li and least for K. It has been proposed that, in the *tert*-butoxide-catalyzed hydrogenation of benzophenone, the reaction is initially catalyzed by *tert*-butoxide, but subsequently by the less reactive benzhydrolate that is formed.[5] Our results are consistent with these observations, indicating that aromatic alkoxides are indeed likely to be less reactive than aliphatic alkoxides.

Table 3. Gibbs Free Energies (ΔG, kJ mol^{-1}) in MOR-Catalyzed Hydrogenation of Formaldehyde[a]

	reaction	MOR	A	B + H$_2$	C[b]	D	E	$\Delta G^{\ddagger}_{cent}$ [c]
gas phase	9	LiO−t-Bu	0	−26	77	−83	−48	103
	10	NaO−t-Bu	0	−16	85	−83	−48	101
	11	KO−t-Bu	0	−15	92	−73	−48	107
solution phase	9	LiO−t-Bu	0	1	149	−24	−62	149[d]
	10	NaO−t-Bu	0	7	145	−40	−62	145[d]
	11	KO−t-Bu	0	−11	126	−54	−62	137

| | | | A | B + H$_2$ | | | D | | | |
	reaction	MOR	closed	open	closed	C[b]	open	closed	E	$\Delta G^{\ddagger}_{cent}$ [c]
gas phase	12	LiOCH$_2$Ph	12	−27	−26	83	−71	−77	−48	110
	13	NaOCH$_2$Ph	−1	−46	−39	76	−91	−81	−48	122
	14	KOCH$_2$Ph	−1	−35	−35	80	−91	−81	−48	115
solution phase	12	LiOCH$_2$Ph	37	8	36	171	−6	7	−62	171[d]
	13	NaOCH$_2$Ph	21	−12	14	153	−37	−11	−62	165
	14	KOCH$_2$Ph	14	−11	−4	131	−41	−33	−62	142

[a] Calculated relative to the reactants **A** (open form of **A** for the benzyloxides). [b] By definition, $\Delta G_{C−A}$ is also the overall barrier of the reaction ($\Delta G^{\ddagger}_{ovr}$). [c] The central barrier is the difference between the free energy of **C** and that of **B** + H$_2$. [d] Because **B** + H$_2$ lies higher in energy than **A**, the central barrier is taken as $\Delta G_{C−A}$ in this case.
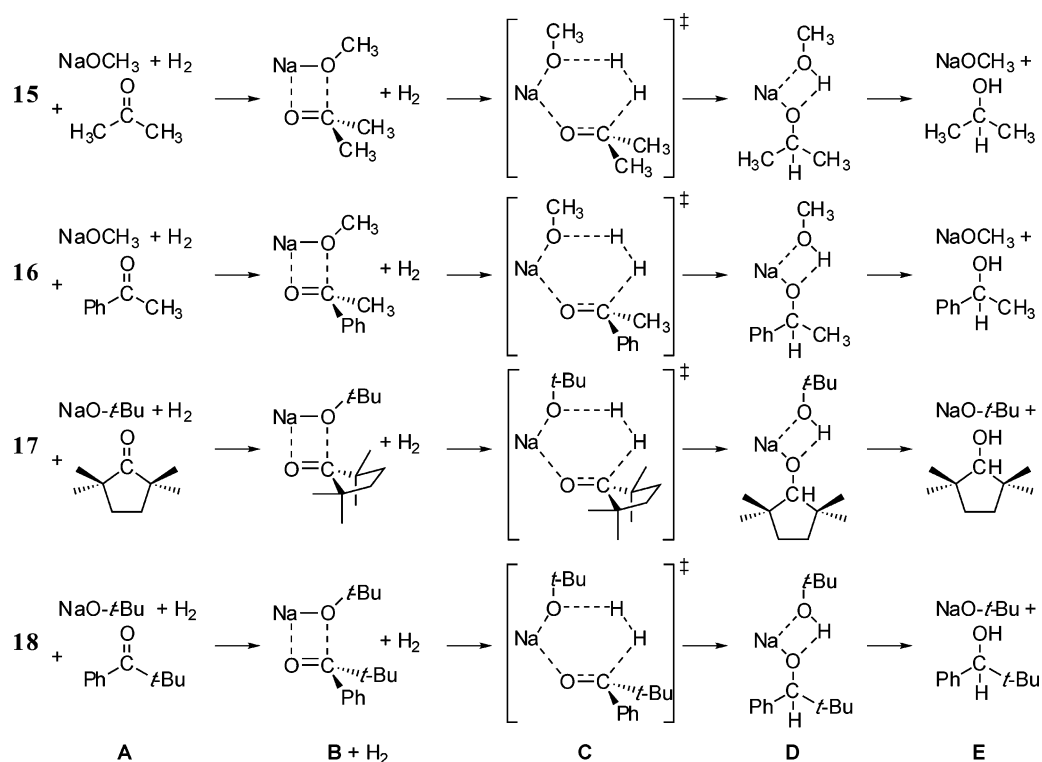
Figure 8. Hydrogenation reactions for acetone (**15**) and acetophenone (**16**) catalyzed by NaOCH$_3$ and hydrogenation reactions for 2,2,5,5-tetramethylcyclopentanone (**17**) and pivalophenone (**18**) catalyzed by Na−O-t-Bu.

Effect of Substrate

It has been observed that aromatic ketones react more readily than aliphatic ketones in base-catalyzed hydrogenation.[5] We have chosen the NaOCH$_3$-catalyzed reactions of acetone and of acetophenone as model systems for the investigation of substrate effects. In addition, we have also examined NaO-t-Bu-catalyzed reactions of 2,2,5,5-tetramethylcyclopentanone and pivalophenone (Figure 8), which are closely related to the reactions investigated by Berkessel.[5]

The ONIOM method was employed for single-point energy calculations for all four reactions, while G3(MP2)-RAD energies were also obtained for the NaOCH$_3$-catalyzed reactions as a reference. The way we partition the species is illustrated in Figure 9 for the transition structures (**C**) of the pivalophenone and 2,2,5,5-tetramethylcyclopentanone reactions.

The real system is treated at the MP2/6-31G(d) level. At the medium level (MP2/G3MP2Large) for reaction **18**, a methyl group is used in place of a *tert*-butyl group, while the phenyl
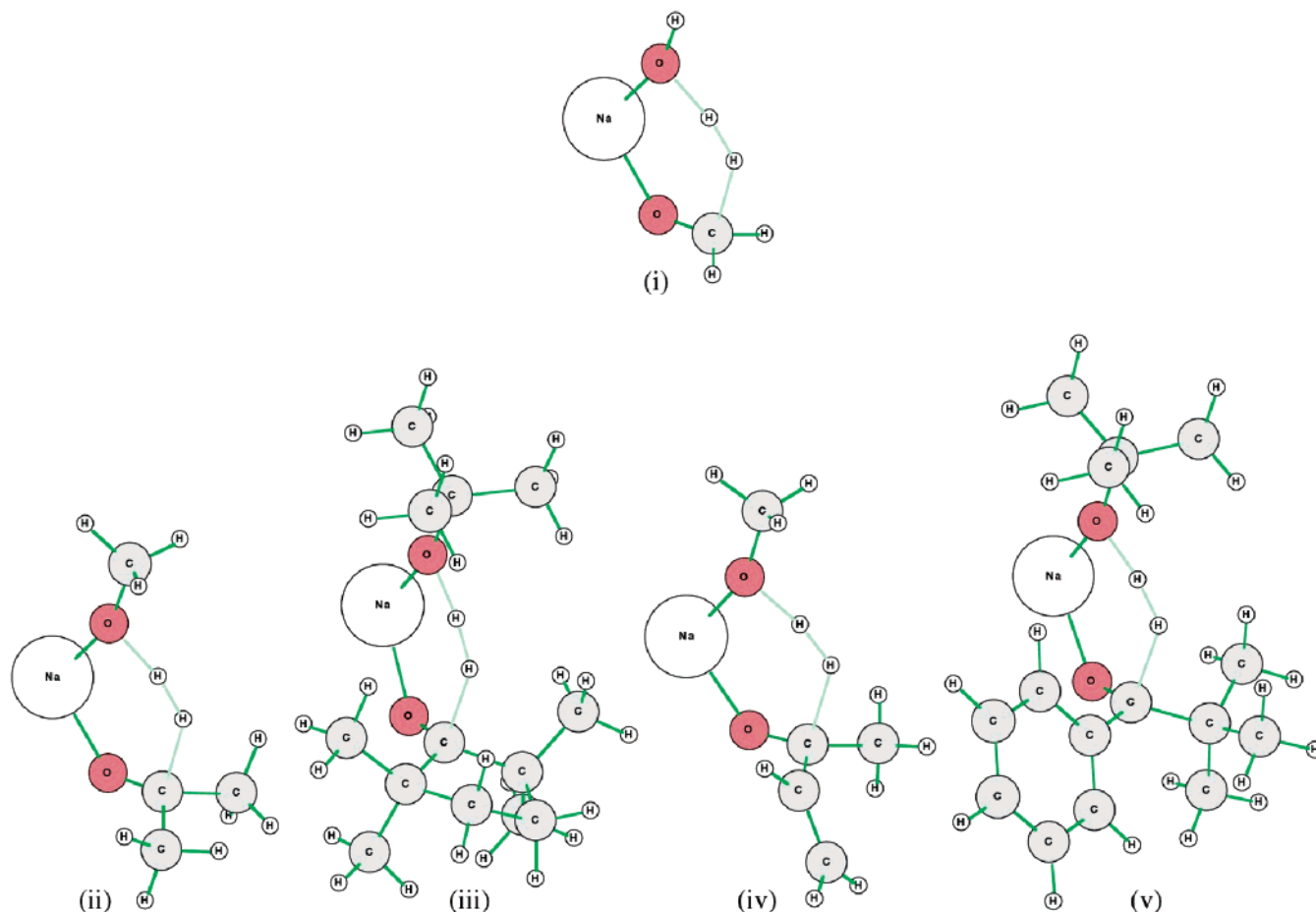
Figure 9. Partition of transition structures (**17C**, **18C**) in ONIOM calculations: (i) model system in both cases; (ii) medium system for **17C**; (iii) real system for **17C**; (iv) medium system for **18C**; and (v) real system for **18C**.

Table 4. Gibbs Free Energies (ΔG, kJ mol^{-1}) in NaOR-Catalyzed Hydrogenation Reactions[a]

	reaction	B + H$_2$	C[b]	D	E	$\Delta G^{\ddagger}_{\text{cent}}$ [c]
gas phase	**15**[d]	−20 (−17)	80 (88)	−51 (−46)	−4 (−3)	100 (105)
	16[d]	−24 (−19)	75 (83)	−68 (−61)	−10 (−9)	99 (102)
	17	−19	107	−33	11	126
	18	−9	91	−75	−26	100
solution phase	**15**	22	149	0	−19	149
	16	24	146	3	−25	146
	17	61	178	32	−6	178
	18	70	162	−1	−42	162

[a] Calculated relative to **A**. ONIOM values unless otherwise specified. [b] By definition, $\Delta G_{\text{C−A}}$ is also the overall barrier of the reaction ($\Delta G^{\ddagger}_{\text{ovr}}$). [c] The central barrier is the difference between the free energy of **C** and that of **B + H$_2$**. [d] G3(MP2)-RAD energies in parentheses.

group is substituted by a vinyl group. 2,2,5,5-Tetramethylcy-clopentanone is treated in a similar way. The high-level layer (CCSD(T)/G3MP2large) for all four reactions comprises NaOH, CH$_2$O, and H$_2$. Other species are treated in the same way as in these examples. Obviously, in constructing the energy profile using the ONIOM method, only two layers are required for some species (e.g., NaOCH$_3$), while H$_2$ is calculated at the CCSD-(T)/G3MP2Large level. The energy profiles for these four reactions are shown in Table 4.

For the two NaOCH$_3$-catalyzed reactions, the ONIOM relative energies are within 8 kJ mol^{-1} of the corresponding G3(MP2)-RAD values. More importantly, the deviations from the G3-(MP2)-RAD energies are consistent for both reactions. For instance, the ONIOM method underestimates the transition structure energies by 8 kJ mol^{-1} for both reactions. Thus, comparison between different reactions using ONIOM energies

is likely to give the same qualitative trends as with G3(MP2)-RAD values.

In the gas phase, the overall barrier for the acetophenone reaction (**16**) is 5 kJ mol^{-1} lower than that for acetone (**15**), while their central barriers are within 1 kJ mol^{-1} of one another. The reactions of 2,2,5,5-tetramethylcyclopentanone (**17**) and pivalophenone (**18**) have somewhat higher overall barriers than those of acetone and acetophenone. However, the aromatic ketone again has a lower overall barrier. Significantly, the difference in overall barriers is 16 kJ mol^{-1}, while the central barrier for the pivalophenone reaction is 26 kJ mol^{-1} lower than that of 2,2,5,5-tetramethylcyclopentanone. The electron-with-drawing phenyl substituent[29] might have an activating effect on the adjacent C=O carbon toward nucleophilic attack. Alternatively, resonance effects[29] could stabilize a charge-separated structure, which would be expected to interact with
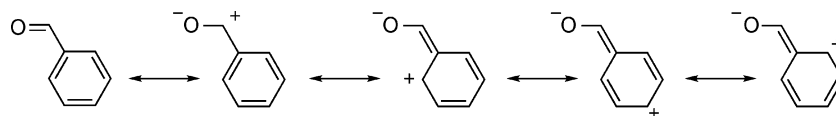
Figure 10. Resonance stabilization associated with charge-separated structures in a phenone.

Table 5. Gibbs Free Energies (ΔG, kJ mol^{-1}) in NaOCH$_3$-Catalyzed Hydrogenation of Formaldehyde in Various Solvents, Obtained Using the IEF-PCM Model[a]

solvent[b]	ϵ[c]	B + H$_2$	C	D	E	$\Delta G^{\ddagger}_{cent}$ [d]
water	78	−29	118	−48	−65	147
methanol	33	−24	123	−43	−62	147
ethanol	25	−25	123	−44	−62	148
isoquinoline	10	−34	110	−55	−63	144
quinoline	9	−32	112	−53	−63	144
THF	8	−30	113	−52	−63	143
aniline	7	−38	104	−61	−67	142
ether	4	−33	106	−58	−61	139
toluene	2	−40	92	−69	−59	132
CCl$_4$	2	−41	90	−71	−59	131
heptane	2	−41	88	−72	−56	129

[a] Calculated relative to **A**. [b] Solvents arranged in descending order of dielectric constant. [c] Dielectric constant of the solvent. [d] The central barrier is the difference between the free energy of **C** and that of **B** + H$_2$.

the catalyst more strongly than the neutral resonance structure (Figure 10).

The fact that the difference in overall/central barriers between the 2,2,5,5-tetramethylcyclopentanone and pivalophenone reactions is larger than that between the acetone and acetophenone reactions indicates the presence of additional factors. Presumably, steric hindrance associated with the four methyl groups might also be contributing to the high barrier for reaction **17**. In solution, the barriers for all four reactions increase by approximately 70 kJ mol^{-1} with respect to the overall gas-phase barriers. This indicates that the effect of solvent on these reactions is relatively uniform, i.e., it is relatively insensitive to minor structural changes in the substrate.

Effects of Solvent

The results presented above indicate that solvation by methanol leads to a higher barrier. To determine the variation in this effect as the solvent is varied, the solution-phase energy profiles for the NaOCH$_3$-catalyzed hydrogenation of formaldehyde with numerous solvents and the IEF-PCM solvation model were examined. The selection of solvent spans a wide range of dielectric constants. We note that some of these solvents might have little practical relevance for base-catalyzed hydrogenations due to poor solubility for the catalyst or chemical incompatibility with strong base. Results for a representative selection of solvents are summarized in Table 5, while the complete set of results is given in the Supporting Information.

It can be seen that the reaction barriers decrease with the dielectric constant of the solvent. In addition, the solvents can be grouped into two categories according to the barriers. With polar solvents, the central barriers lie in the 139−148 kJ mol^{-1} range, while, for nonpolar (or nearly nonpolar) solvents, the central barriers lie in the 129−132 kJ mol^{-1} range. Using a nonpolar solvent such as heptane could theoretically give rise

(29) For general information on inductive and resonance effects, see: (a) Swain, C. G.; Lupton, E. C., Jr. *J. Am. Chem. Soc.* **1968**, *90*, 4328. (b) Exner, O. *J. Phys. Org. Chem.* **1999**, *12*, 265. (c) Smith, M. B.; March, J. *Advanced Organic Chemistry: Reactions, Mechanisms, and Structure*, 5th ed.; Wiley: New York, 2001.

to the most rapid reaction. In practice, however, the metal cation is likely to be insoluble in such solvents. Nevertheless, a carefully chosen solvent with a good balance between solvent polarity and catalyst solubility could potentially provide an improvement in the observed reactivity. A polar solvent with a small dielectric constant, such as diethyl ether, could be a sensible choice.

Concluding Remarks

Ab initio molecular orbital calculations have been applied to the study of the base-catalyzed hydrogenation of carbonyl compounds. The results are qualitatively in accord with a recent experimental study.[5] The following important points emerge from the present study:

1. Base-catalyzed hydrogenation reactions share many common features with S$_N$2 reactions. Both types of reaction are described by double-well energy profiles. At 0 K, the gas-phase reactions have deep wells and a low or negative overall energy barrier. On the other hand, solution-phase profiles show very shallow wells and much higher barriers.

2. There is a large entropic contribution to the barriers, indicating that the assembly of the highly ordered transition structure is a major factor in limiting the rate of reaction.

3. In the gas phase, the overall barrier for the hydrogenation of formaldehyde catalyzed by Group I to Group III methoxides varies widely with the metal. For Group I metals, the overall barriers increase steadily down the group. We have attributed this to the decreasing charge density as the size of the metal increases. On the other hand, for Group II and Group III metals, the overall barriers decrease down the group, which is attributed to the increasing ionic character down the group. The reaction with B(OCH$_3$)$_3$ has an exceptionally high barrier, which is attributed to its high covalency and to π-electron donation from the oxygen lone pairs of the methoxy groups to the formally vacant p orbital on boron, which weakens interaction with the substrate.

4. In solution, the reactivity trends are generally the opposite of the corresponding gas-phase trends. Thus, for this type of base-catalyzed hydrogenation, the effect of solvation on the catalysts is a dominating factor in the catalytic activity. This observation is also similar to that pertaining to solution-phase S$_N$2 reactions, in which the degree of solvation of the nucleophile overrides the gas-phase reactivity.

5. Substituting methoxides by *tert*-butoxides does not lead to a large change in solution-phase barriers. However, when benzyloxides are used as catalysts, the barriers are predicted to be larger, both in the gas phase and in solution.

6. Aromatic ketones are likely to be more reactive than purely aliphatic ketones. Comparison between catalytic hydrogenation of 2,2,5,5-tetramethylcyclopentanone and of pivalophenone shows that factors such as steric effects may also be important in differentiating their reactivity.

7. Solvation studies with a wide range of solvents indicate a steady decrease in barrier with solvent dielectric constant. In particular, nonpolar solvents generally lead to considerably lower

barriers than polar solvents. In practice, however, the base catalyst is unlikely to be soluble in a nonpolar solvent. A good balance between polarity and catalyst solubility is therefore required in selecting the optimum solvent for the base-catalyzed hydrogenation reaction.

Supporting Information Available: GAUSSIAN 03 archive entries for B3-LYP/6-31G(d)-optimized geometries of relevant equilibrium structures and transition structures, calculated G3-(MP2)-RAD and ONIOM(CCSD(T)/G3MP2Large:MP2/G3MP2Large: MP2/6-31G(d)) total energies, B3-LYP/6-31G(d) solution phase (IEF-PCM) relative energies, and B3-LYP/6-31G(d) IEF-PCM energies of solvation. This material is available free of charge via the Internet at http://pubs.acs.org.

JA0450253